



Article

Reducing energy barriers of chemical reactions with a nanomicrocell catalyst consisting of integrated active sites in conductive matrices

Guo-Peng Zhan, Chuan-De Wu*

State Key Laboratory of Silicon Materials, Center for Chemistry of High-Performance & Novel Materials, Department of Chemistry, Zhejiang University, Hangzhou 310027, China

ARTICLE INFO

Article history:

Received 25 January 2019

Received in revised form 30 January 2019

Accepted 3 February 2019

Available online 23 February 2019

Keywords:

Nanomicrocell catalysts

Conductive matrices

Electrode pairs

Electrolytes

Primary cells

ABSTRACT

Reducing energy barriers of chemical reactions is the never-ending endeavor of chemists. Inspired by the high reactivity of primary cells, we develop a nanosized fuel cell catalyst (denoted as nanomicrocell catalyst), consisting of integrated electrode pairs, conductive matrices and electrolytes, to improve the chemical reactivity. Specifically, the anodes are Pd species which is combining with the electron-rich N atoms in B-and-N co-doped carbon dots; the cathodes are electron-deficient B atoms; and the conductive matrices are B-and-N co-doped carbon dots which are connecting with the electrode pairs. Similar to the reactivity of primary cells, the catalytic properties of the nanomicrocell catalyst in hydrogenation of benzaldehyde are depending on the properties of electrode pairs, conductive matrices and electrolytes. The unique catalytic properties are attributed to the different substrate adsorption capability and catalytic properties of paired electrodes, and the easy migration of electrons and charge carriers, which could improve the synergetic effect between paired active sites. Therefore, this work may open up a new window for designed synthesis of advanced catalysts which could highly lower the energy barriers of chemical reactions.

© 2019 Science China Press. Published by Elsevier B.V. and Science China Press. All rights reserved.

1. Introduction

Chemical reactions are involving electron transfer between different atomic sites, depending on their chemical potentials. In other word, there exists directional movement of electrons between different atomic sites in chemical reactions, which can be viewed as the smallest batteries. Because there are energy barriers in chemical reactions, the directional movement of electrons is often hindered, even though the Gibbs free energies of reactions are highly negative. To overcome the energy barriers, most chemical reactions have to be performed under harsh conditions to jump across energy barriers or in the presence of catalysts to lower energy barriers by alternating the reaction paths. Thus, more than 90% of industrial processes, including chemical, petrochemical and biochemical processes, require homo- or heterogeneous catalysts [1].

There are many electronic devices, such as primary cells [2], fuel cells [3], lithium batteries [4] and supercapacitors [5], which endow long-range directional movement of electrons between different atomic sites on separated electrode pairs for chemical reactions. These devices can not only directly transfer chemical energy into electric energy but also render the chemical reactions more

reactive, compared with traditional catalytic reactions. These results suggest that immobilization of different active sites in electrode pairs could accelerate reaction rates. It is worth noting that the long-range directional movement of electrons and charge carriers in chemical reactions has widely existed in the nature by forming small primary cells, such as steel corrosion [6] and physiological processes [7]. The reactivity of these small batteries is depending on the relative chemical potentials of electrode pairs which could induce long-range directional movement of electrons and charge carriers. For example, there are many spontaneous small primary cells on steel surfaces in the presence of impurity carbon species, consisting of iron anodes and carbon cathodes (Fig. 1a). Under basic or neutral moisture conditions in the air, there are two half-reactions for iron anodes ($\text{Fe} - 2\text{e} = \text{Fe}^{2+}$) and carbon cathodes ($1/2\text{O}_2 + \text{H}_2\text{O} + 2\text{e} = 2\text{OH}^-$). The electron transfer would be directionally induced from anodes to cathodes through metallic iron, controlled by the different chemical potentials of carbon cathodes and iron anodes. Meanwhile, the resultant OH^- ions would be directionally migrated from cathodes to anodes, and vice versa for Fe^{2+} ions. As a consequence, metallic iron was oxidized into $\text{Fe}(\text{OH})_2$ and further oxidized into $\text{Fe}_2\text{O}_3 \cdot n\text{H}_2\text{O}$. The corrosion rate would be accelerated under high moisture or high salinity conditions. However, the iron corrosion rate would be decelerated under high-purity iron and/or under drying conditions which make it difficult to form reactive primary cell. These results indicate that

* Corresponding author.

E-mail address: cdwu@zju.edu.cn (C.-D. Wu).

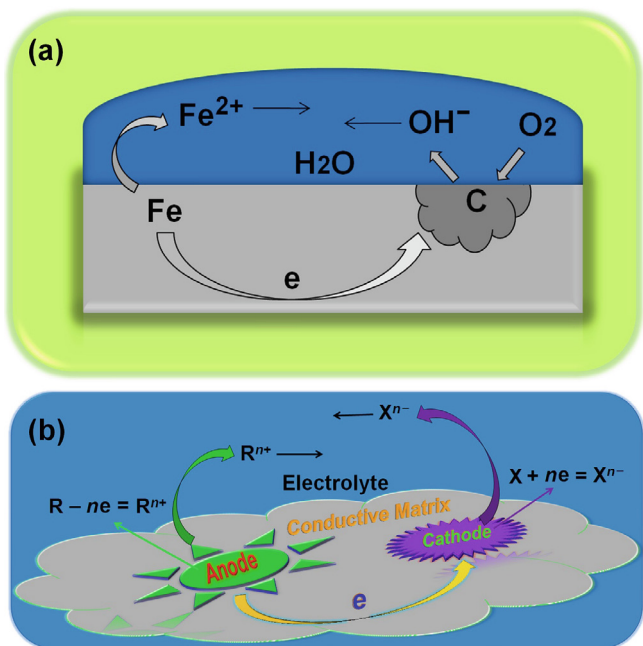


Fig. 1. (Color online) (a) Schematic representation of the iron corrosion process under basic or neutral moisture conditions in the air. (b) Schematic representation of the proposed nanomicrocell catalyst system.

primary cell system could tune the energy barriers of chemical reactions and modulate the reaction rates.

These observations inspired us to develop a proof-of-concept nanosized fuel cell catalyst (denoted as nanomicrocell catalyst) to improve the efficiency of catalysis. Similar to fuel cells, the nanomicrocell catalyst consists of nanosized anodes and cathodes that are connected by nanosized conductive matrices. According to the electron current direction from anodes to cathodes, the anodes should preferably combine with reductive molecules, and the cathodes should selectively combine with oxidative molecules. Accordingly, we synthesized boron-and-nitrogen co-doped carbon dots (denoted as BNCD) as hybrid conductive matrices, which were further reacted with PdCl_2 to generate an integrated nanomicrocell catalyst (denoted as Pd-BNCD). In Pd-BNCD, the anodes are Pd species that is combined with electron-rich nitrogen atoms; the cathodes are electron-deficient boron atoms; and the conductive matrices are hybrid carbon dots BNCD, which are connected with the electrode pairs. The nanomicrocell catalyst Pd-BNCD exhibits high catalytic efficiency in hydrogenation of benzaldehyde in the presence of acidic electrolyte. The catalytic properties of Pd-BNCD are much more efficient than those of control catalysts without effective electrode pairs. The catalytic properties of the nanomicrocell catalyst are also depending on electrolytes, such as acidic, basic and neutral electrolytes, which can affect the migration of charge carriers and activation of reactant molecules.

2. Experimental

2.1. Materials and methods

All chemicals are analytical grade, which were obtained from commercial sources and were used without further purification. FT-IR spectra were collected from KBr pellets on an FTS-40 spectrophotometer. Elemental analyses were performed on a ThermoFinnigan Flash EA 1112 element analyzer. GC-MS spectra were recorded on a SHIMADZU GCMS-QP2010. Inductively coupled plasma mass spectrometry (ICP-MS) was performed on an X-Series

II instrument. X-ray photoelectron spectra (XPS) were measured by a Kratos AXIS Supra with Al $K\alpha$ irradiation (1,486.6 eV), and the binding energies were calibrated using the C 1s peak at 284.6 eV. Transmission electron microscopy (TEM) equipped with an energy dispersive X-ray (EDX) detector was recorded on a JEM 2100F equipment, and the samples were deposited onto ultrathin carbon films on carbon grids. Electron paramagnetic resonance (EPR) spectra were recorded on a Bruker ESRA-300 at room temperature.

2.2. Synthesis of Pd-BNCD

Pd-BNCD was synthesized according to a slightly modified literature procedure [8]. Citric acid (7.65 mmol), disodium edetate (3.825 mmol) and *p*-carboxyphenylboronic acid (3.825 mmol) were dissolved in 35 mL water in a flask. The mixture was sonicated and dispersed uniformly in an ultrasonic cleaner for 30 min, which was subsequently transferred into a 50 mL Teflon autoclave and heated at 200 °C for 5 h. After the mixture was naturally cooled to room temperature, the resulting boron-and-nitrogen co-doped carbon dot solution was collected by centrifugation to remove large particles of insoluble matter. PdCl_2 (0.95 mmol) was added into the supernate, which was heated at 100 °C under stirring for 12 h, and cooled to room temperature. A solid powder sample of Pd-BNCD was obtained by rotary evaporation under reduced pressure.

2.3. Catalytic activity measurement

The hydrogenation reduction of benzaldehyde was carried out in a 10 mL Schlenk tube equipped with a magnetic stir bar. In a typical experiment, benzaldehyde (0.3 mmol), HBF_4 (0.08 mmol), Na_2SO_4 (0.02 mmol) and catalyst (1.5 μmol based on the content of Pd species) in acetonitrile (1 mL) in the Schlenk tube were stirred under H_2 atmosphere (balloon) at 25 °C for 2 h. The identity of products was determined by GC-MS, and compared with the authentic samples analyzed under the same conditions, while the conversion of benzaldehyde, and the yields and selectivity of products were obtained by GC analysis using a flame-ionization detector (FID) with a capillary SE-54 column.

3. Results and discussion

Yellow colored boron-and-nitrogen co-doped carbon dots (denoted as BNCD) were synthesized by hydrothermal condensation reaction of a mixture of citric acid (carbon source), disodium edetate (nitrogen source) and *p*-carboxyphenylboronic acid (boron source). BNCD was subsequently metalated with PdCl_2 to generate a composite material as a nanomicrocell catalyst (denoted as Pd-BNCD). In the FT-IR spectrum of BNCD, the weak peak at $1,130\text{ cm}^{-1}$ corresponds to the stretching vibration of C–B bonds, and the peak at $1,048\text{ cm}^{-1}$ corresponds to the stretching vibration of C–N bonds, indicating that boron and nitrogen elements were successfully doped in BNCD (Fig. S1 online) [9]. The morphology of Pd-BNCD was characterized by transmission electron microscopy (TEM) and high-resolution transmission electron microscopy (HRTEM). As shown in Fig. 2, the sizes of Pd-BNCD are around 2–5 nm, and the lattice spacing is well matched with that of graphene [10]. There is no aggregated Pd nanoparticle according to the TEM and HRTEM images of Pd-BNCD, indicating that the Pd species was immobilized on BNCD by coordinating to the nitrogen atoms. This conclusion was confirmed by monitoring high-angle annular dark-field scanning transmission electron microscopy (HAADF-STEM) image, energy dispersive X-ray spectroscopy and electron paramagnetic resonance (EPR) spectroscopy (Fig. S2 online). The composition of Pd-BNCD was studied by ICP-MS and

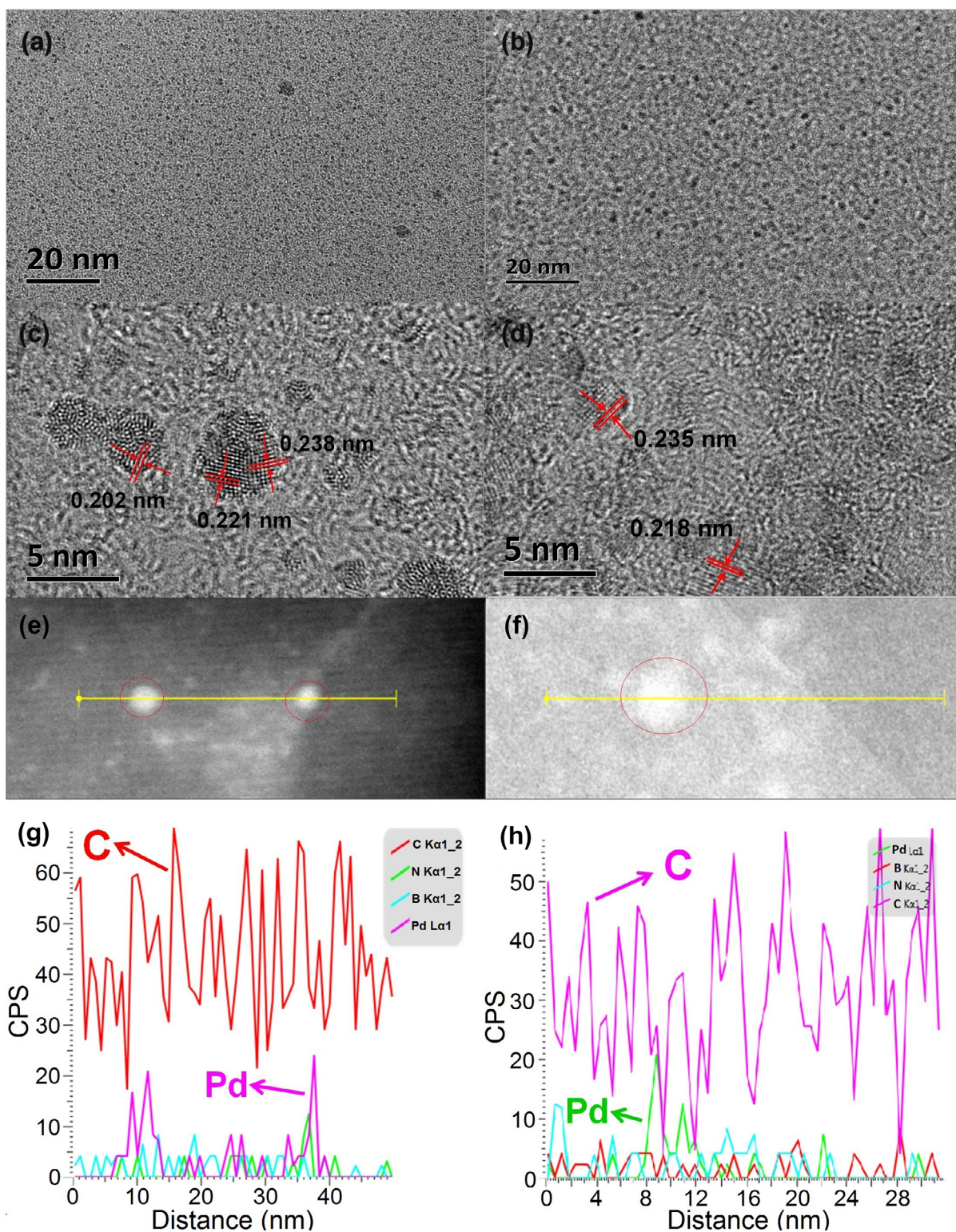


Fig. 2. (Color online) TEM (a, b), HRTEM (c, d) and HAADF-STEM (e, f) images, and energy dispersive X-ray spectra (g, h) for the nanomicrocell catalyst Pd-BNCD before (left column) and after (right column) catalysis.

elemental analysis (Table S1 online). There are about 3.13% Pd, 1.08% B and 4.19% N with the Pd, B and N ratio of about 1:3:9 in Pd-BNCD.

The chemical compositions of BNCD and Pd-BNCD were further characterized by monitoring the electronic states of Pd, N, B and C in X-ray photoelectron spectroscopy (XPS). As shown in Fig. 3, both samples contain abundant C element and relatively low contents of

B, N, O and/or Pd elements. In the high-resolution B 1s XPS spectra of BNCD and Pd-BNCD, the peak centered at 192.1 eV corresponds to the boronic acid moiety (CBO₂) [11]. The high resolution N 1s XPS spectrum of BNCD is overlapped by two peaks, which should be ascribed to the pyrrolic nitrogen (399.55 eV) and graphitic nitrogen (401.60 eV) atoms. The XPS peaks for N 1s in Pd-BNCD are slightly shifted to 399.2 and 401.2 eV, which should be

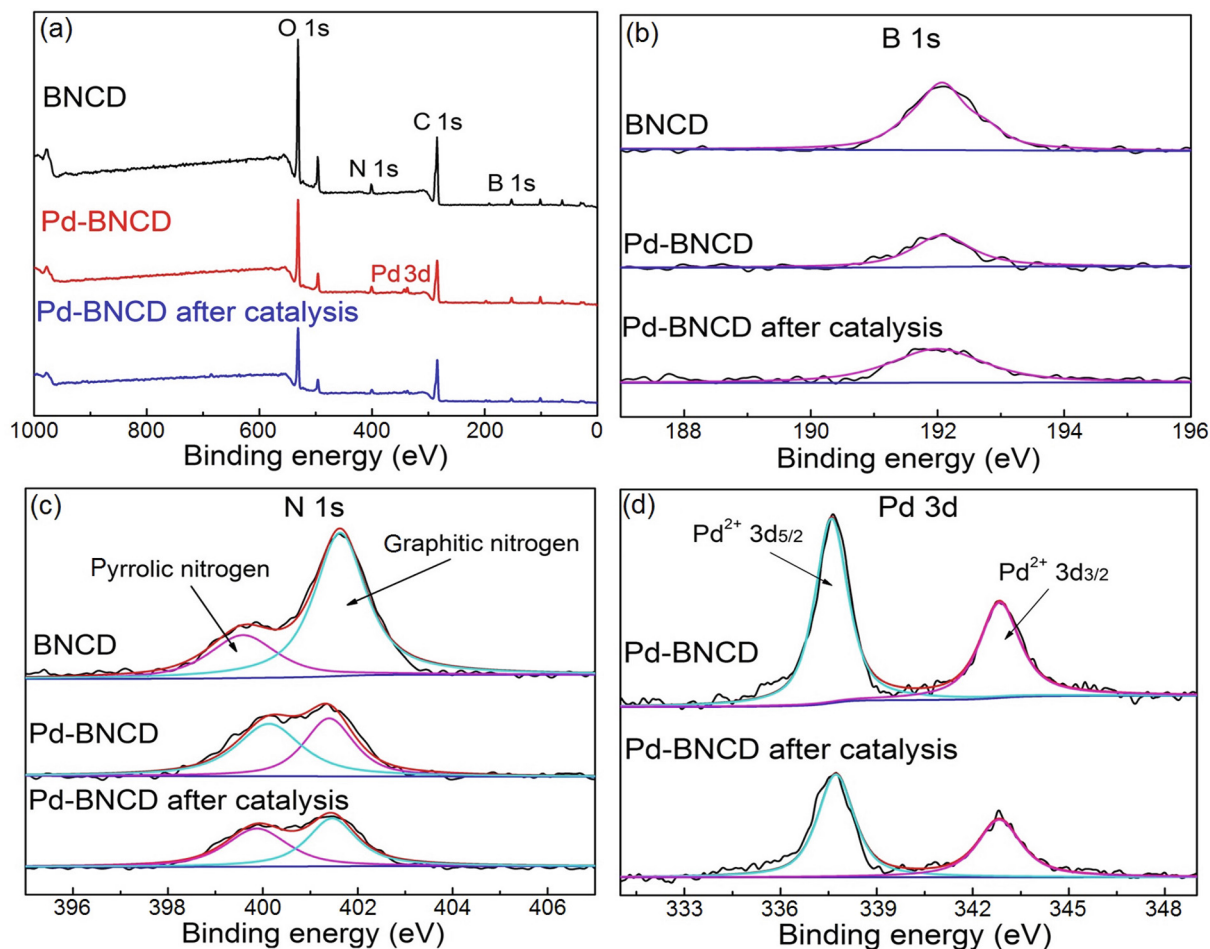


Fig. 3. (Color online) (a) The XPS survey spectra of BNCD and Pd-BNCD, and the high-resolution (b) B 1s, (c) N 1s and (d) Pd 3d XPS spectra for BNCD and Pd-BNCD.

attributed to the coordination of nitrogen to Pd atoms [12]. In the high-resolution Pd 3d XPS spectrum of Pd-BNCD, the peaks centered at 337.6 and 342.8 eV are related to Pd^{II} 3d_{5/2} and 3d_{3/2}, respectively. Compared with those values for PdCl₂ (338.0 eV for 3d_{5/2} and 343.7 for 3d_{3/2}), the peaks are negatively shifted, which indicates that the Pd^{II} species is coordinating to the electron-rich nitrogen atoms in Pd-BNCD [13].

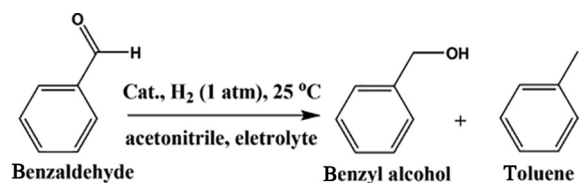
According to the reactivity of primary cells, the catalytic properties of nanomicrocell catalysts should be controlled by the chemical potentials, reactant adsorption capability and catalytic properties of electrode pairs, and the directional migration capability of electrons, charge carriers and reaction intermediates, which should be the characters of nanomicrocell catalysts. We selected catalytic hydrogenation of benzaldehyde as a model reaction to illustrate the roles of different elements of the nanomicrocell catalyst Pd-BNCD. Additionally, to demonstrate the roles of electrolytes, three different conditions were set in the catalytic reaction, including acidic, basic and neutral conditions.

The catalytic hydrogenation reaction was performed in acetonitrile at room temperature (25 °C) under 1 atm H₂ atmosphere (balloon). As shown in Table 1, the hydrogen reaction catalyzed by the nanomicrocell catalyst Pd-BNCD is almost complete in 2 h under acidic conditions (entry 1). Under the identical conditions, the conversion of benzaldehyde is of 11.2% catalyzed by PdCl₂ (entry 2). The improved catalytic efficiency of Pd-BNCD should be attributed to the formation of nanomicrocell system, which could reduce the energy barrier of the reduction reaction. To understand the roles of electrodes, we synthesized a series of carbon materials, including

carbon dots (CDs), nitrogen-doped carbon dots (NCDs) and boron-doped carbon dots (BCDs), which were subsequently metalated with PdCl₂ to generate Pd-CD, Pd-NCD and Pd-BCD composite materials as control catalysts (Figs. S3–S8 online). Under the identical conditions, the conversion of benzaldehyde catalyzed by the control catalyst Pd-NCD is undetectable (entry 3), whereas the conversions are of 12.9% and 7.2% catalyzed by Pd-CD and Pd-BCD, respectively (entries 4 and 5). These results indicate that electrodes played important roles in the catalytic reaction, which could selectively activate different reactant molecules to prompt long-range directional electron transfer between different atomic sites. We further studied the effect of electrolytes on the catalytic efficiency (Fig. S9 online). The catalytic efficiency of Pd-BNCD catalyst under acidic conditions is much higher than that under basic or neutral conditions (entries 1, 6 and 7). These results indicate that protons acted not only as positive charge carriers but also as reactive intermediates to directly activate and react with the reactant molecules. When mixed catalysts Pd(bpy)Cl₂/BCD and Pd-NCD/BPBA (BPBA = (4-(naphthalen-1-yl)phenyl)boronic acid) were used instead of Pd-BNCD under the identical conditions, the conversions of benzaldehyde are of 1.8% and 18.9%, respectively (entries 8 and 9). These results indicate that the conductive matrices also played important roles in the hydrogenation reaction.

According to the catalytic results, we proposed a plausible catalytic cycle for the reduction reaction catalyzed by the nanomicrocell catalyst (Scheme 1). At first, the Pd^{II} species, immobilized on the nitrogen atoms in BNCD, would preferably adsorb molecular hydrogen and be reduced to Pd⁰. The Pd⁰ species would further

Table 1
Catalytic hydrogenation of benzaldehyde under mild conditions.^a



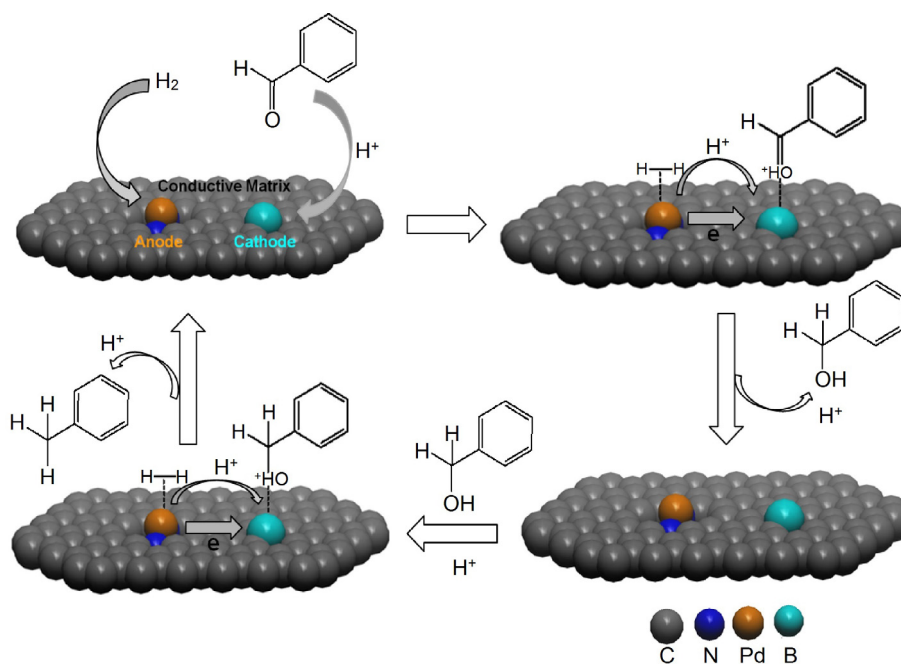
Entry	Catalyst	Electrolyte	Conversion (%) ^b	Selectivity (%) ^b	
				Toluene	Benzyl alcohol
1	Pd-BNCD	HBF ₄	>99	93.6	6.4
2	PdCl ₂	HBF ₄	11.2	>99	Trace
3	Pd-NCD	HBF ₄	Trace	–	–
4	Pd-CD	HBF ₄	12.9	>99	Trace
5	Pd-BCD	HBF ₄	7.2	17.5	82.5
6	Pd-BNCD	–	Trace	–	–
7	Pd-BNCD	Na ₂ CO ₃	Trace	–	–
8	Pd(bpy)Cl ₂ /BCD	HBF ₄	1.8	25.0	75.0
9	Pd-NCD/BPBA	HBF ₄	18.9	91.5	8.5

^a Reaction conditions: catalyst (1.5 μmol based on the content of Pd species), benzaldehyde (0.3 mmol), Na₂SO₄ (0.02 mmol) and HBF₄ (0.08 mmol) or Na₂CO₃ (0.01 mmol) in acetonitrile (1 mL) were stirred at room temperature (25 °C) under an atmosphere of H₂ (balloon) for 2 h.

^b Determined by GC–MS.

adsorb molecular hydrogen, which has the potential to cleavage the H–H bond for the formation of H[•] species. The electron-deficient B cathode could preferably combine with the electron-rich oxygen atom of benzaldehyde by forming C=O···B bond through Lewis base and acid interaction. The oxygen atom in C=O···B is easily protonated under acidic conditions, which could increase polarization of the C=O bond. Induced by the different chemical potentials of the electrode pairs, the electrons would be inclined to directionally migrate from Pd/N anode to B cathode through the conductive backbone of BNCD. The synergistic effect between palladium and boron sites could synchronously prompt activation of hydrogen and substrate molecules, respectively. As

a result, H[•] species on Pd/N anode was oxidized to protons. The released electrons were injected into the hybridized sp²-carbon backbone of BNCD and further transferred to the cathode B site which lead to the reduction of C=OH⁺ moiety in protonated benzaldehyde. As a result, benzaldehyde was reduced to benzyl alcohol. After the resultant protons were directionally migrated from anode to cathode, the catalytic cycle was closed. When the hydroxyl group in benzyl alcohol is further combined with the B cathode and protonated, benzyl alcohol would be further reduced to toluene. If there is no suitable electrolyte that consists of desired ions to activate the reactant molecules and complete the electronic cycle, the nanomicrocell catalyst almost does not work. The



Scheme 1. (Color online) Proposed catalytic cycles for hydrogenation reduction of benzaldehyde catalyzed by the nanomicrocell catalyst Pd-BNCD.

catalytic efficiency of Pd-CD, Pd-NCD and Pd-BCD catalysts is very low, because these catalysts are lack of efficient electrode pairs to induce the electron and charge transfer. The catalytic activity of Pd-BCD is higher than that of Pd-NCD, which should be ascribed to the lack of electron-deficient B site as cathode in Pd-NCD that could induce directional electron transfer from Pd site to protonated benzaldehyde. Due to the lack of nitrogen site to effectively combine with the palladium species in Pd-BCD, the catalytic efficiency is very low. Moreover, as the Pd species in Pd-BCD cannot effectively interact with the conductive backbones for electron transfer, the catalytic properties of Pd-BCD are much inferior to those of the nanomicrocell catalyst Pd-BNCD.

4. Conclusions

In summary, we demonstrated a proof-of-concept nanomicrocell catalyst Pd-BNCD, composed of integrated Pd species and boron-and-nitrogen co-doped carbon dots, to illustrate the catalytic properties and mechanism of nanomicrocell catalysts. Similar to the primary cells, the nanomicrocell catalyst system consists of electrode pairs (electron-rich Pd/N anodes and electron-deficient B cathodes), conductive matrices (BNCD) and electrolytes (acid). The catalytic efficiency of the nanomicrocell catalyst system in hydrogenation of benzaldehyde is controlled by the chemical potentials and the catalytic properties of electrode pairs, which could strip and capture electrons, and further induce directional charge transfer between different active sites. The conductivity of hybrid carbon backbones and the reactivity of electrolytes are also very important in the catalytic reaction, which could synergistically prompt activation of reactant molecules. Compared with traditional catalysts, the advantage of the nanomicrocell catalyst system lies in the active sites with different catalytic properties that are separately designed and synthesized according to the specific half-reactions. The electrode pairs played different roles in the catalytic hydrogenation reaction by selectively reacting with different reactant molecules. Given the wide scope of chemical reactions that are involving electron transfer, this work sheds new light on the general design principles for nanomicrocell catalysts toward the chemical reactions with high energy barriers by rationally integrating different active sites in electrode pairs on conductive matrices, and directly correlating the catalytic properties of electrode pairs with different half-reactions.

Conflict of interest

The authors declare that they have no conflict of interest.

Acknowledgments

This work was supported by the National Natural Science Foundation of China (21373180, 21525312, and 21872122).

Author contributions

Chuan-De Wu conceived the idea and guided the whole project. Guo-Peng Zhan designed and performed the experiments. Guo-Peng Zhan and Chuan-De Wu analyzed the data and co-wrote the manuscript.

Appendix A. Supplementary material

Supplementary data to this article can be found online at <https://doi.org/10.1016/j.scib.2019.02.004>.

References

- [1] Gucci L, Erdöhelyi A. Catalysis for alternative energy generation. New York: Springer; 2012.
- [2] Park J, Park M, Nam G, et al. All-solid-state cable-type flexible zinc-air battery. *Adv Mater* 2014;27:1396–401.
- [3] Huang XQ, Zhao ZP, Cao L, et al. High-performance transition metal-doped Pt₃Ni octahedra for oxygen reduction reaction. *Science* 2015;348:1230–4.
- [4] Li Z, Ma ZL, Wang YY, et al. LDHs derived nanoparticle-stacked metal nitride as interlayer for long-life lithium sulfur batteries. *Sci Bull* 2018;63:169–75.
- [5] Gao XY, Li XY, Kong Z, et al. Bifunctional 3D n-doped porous carbon materials derived from paper towel for oxygen reduction reaction and supercapacitor. *Sci Bull* 2018;63:621–8.
- [6] Lazzari L, Pedferri MP. Corrosion science and engineering. Cham: Springer International Publishing; 2018.
- [7] Zannoni D, Philippis RD. Microbial bioenergy: hydrogen production. Dordrecht: Springer; 2014.
- [8] Zhu SJ, Meng QN, Wang L, et al. Highly photoluminescent carbon dots for multicolor patterning, sensors, and bioimaging. *Angew Chem Int Ed* 2013;52:3953–7.
- [9] Zhang YM, Zhao JH, Sun HL, et al. B, N, S, Cl doped graphene quantum dots and their effects on gas-sensing properties of Ag-LaFeO₃. *Sens Actuat B* 2018;266:364–74.
- [10] Chua CK, Sofer Z, Simek P, et al. Synthesis of strongly fluorescent graphene quantum dots by cage-opening buckminsterfullerene. *ACS Nano* 2015;9:2548–55.
- [11] Fan Z, Li Y, Li X, et al. Surrounding media sensitive photoluminescence of boron-doped graphene quantum dots for highly fluorescent dyed crystals, chemical sensing and bioimaging. *Carbon* 2014;70:149–56.
- [12] Chen ZY, Wang QC, Zhang XB, et al. N-doped defective carbon with trace Co for efficient rechargeable liquid electrolyte/all-solid-state Zn-air batteries. *Sci Bull* 2018;63:548–55.
- [13] Militello MC, Simko SJ. Palladium chloride (PdCl₂) by XPS. *Surf Sci Spectra* 1994;3:402–9.



Guo-Peng Zhan received his B.S. degree in Chemistry from Zhejiang University in 2017. Currently, he is a graduate student in Chemistry Department of Zhejiang University under the guidance of Professor Chuan-De Wu. His research work is focused on the development of nanomicrocell catalysts and catalytic applications.



Chuan-De Wu is Qiushi Professor of Zhejiang University. He obtained his Ph.D. degree in Physical Chemistry from Fujian Institute of Research on the Structure of Matter, Chinese Academy of Sciences in 2003. He worked as a postdoctoral fellow at the University of North Carolina at Chapel Hill during 2003–2005 before joining Zhejiang University in 2005 as a full professor of chemistry. His research interest focuses on the development of biomimetic framework materials and new proof-of-concept catalysts for catalytic applications.